Available online at www.sciencedirect.com

ScienceDirect

Journal of Taibah University for Science 8 (2014) 137–141

Journal of Taibah University for Science

www.elsevier.com/locate/jtusci

Equation of state model for studying high-pressure compression behaviour of nanomaterials

Kuldeep Kholiya [a,*], Jeewan Chandra [b]

[a] *Department of Applied Science, B.T. Kumaon Institute of Technology, Dwarahat 263653, India*
[b] *Department of Applied Science, G.B. Pant Engineering College Ghurdauri, Pauri Garhwal 246194, India*

Received 23 July 2013; received in revised form 22 September 2013; accepted 30 September 2013
Available online 24 October 2013

Abstract

The high-pressure compression behaviour of the nanomaterials 3C-SiC, $Zr_{0.1}Ti_{0.9}O_2$, CuO, AlN, TiO_2 (anatase), TiO_2 (rutile), α-Fe_2O_3, γ-Fe_2O_3, ε-Fe and Rb_3C_{60} was studied in two theoretical equation of state (EOS) models. In the first model, we considered the pressure to be quadratic in terms of relative volume change, while in the second model pressure was considered to be quadratic in density. The experimental data show that the second model gives better results. The two models were also studied for their suitability in cases of very high compression.

PACS: 64.10.+h; 62.20.−x; 62.20.de

Keywords: Equation of state; High pressure; Nanomaterial; Bulk modulus; Pressure derivative

1. Introduction

Nanomaterials are undergoing rapid development because of their potential applications in areas such as electronics, catalysis, ceramics, magnetic data storage and structural components. Studies of the compressibility and pressure-induced phase transitions of nanocrystalline materials could improve our understanding of the stable state of materials down to the nanometre scale. Most research on high-pressure nanocrystalline materials has been conducted on semiconductors, although work on insulators and metals was reported recently. The effects of applying high pressure to nanomaterials include transformation of nano-constitutive elements, transformation of the interactions between nano objects and modification of interactions between nano objects and the pressure-transmitting medium.

Liu et al. [1] synthesized nanocrystalline 3C-SiC (30 nm) by laser-induced vapour-phase reactions and performed an energy dispersive X-ray diffraction experiment at room temperature, with silicon oil as the pressure-transmitting medium to obtain a quasi-hydrostatic condition. They observed a decrease in the Born transverse effective charge of these nanocrystals with increasing pressure, in contrast to its bulk counterpart. Holbig et al. [2] studied the compression behaviour of Zr-doped nanoanatase $Zr_{0.1}Ti_{0.9}O_2$ synthesized by the sol gel method in a diamond anvil cell and found no evidence of phase transition up to a pressure of 13 GPa. Wang et al. [3] studied the EOS of nanocrystalline

* Corresponding author. Tel.: +91 7895563339.
E-mail address: kuldeep_phy1@rediffmail.com (K. Kholiya).
Peer review under responsibility of Taibah University

ELSEVIER Production and hosting by Elsevier

1658-3655
http://dx.doi.org/10.1016/j.jtusci.2013.09.007

CuO (24 nm) by high-energy synchrotron radiation and Raman spectroscopy, and Wang et al. [4] studied AlN nanocrystals under hydrostatic conditions up to a pressure of 36.9 GPa with an energy-dispersive synchrotron radiation technique in a diamond anvil cell. Shen et al. [5] investigated the structural transition of AlN nanowires by in situ angle dispersive high-pressure X-ray diffraction with a synchrotron radiation source and found pressure-induced wurtzite-to-rocksalt phase transition at 45.4 GPa. Swamy et al. [6] reported a synchrotron X-ray diffraction study of pressure-induced changes in nanocrystalline anatase TiO_2 (with a crystallite size of 30–40 nm) to 35 GPa and found that the bulk modulus value for nanocrystalline anatase is about 35% greater than that of the macrocrystalline material. Olsen et al. [7] studied the high-pressure behaviour of nanocrystalline rutile TiO_2 at ambient temperature by X-ray diffraction and found that it is transformed to the monoclinic baddeleyite structure at 20–30 GPa. Clark et al. [8] observed a pressure-induced structural phase transition of γ-Fe_2O_3 (maghemite) to α-Fe_2O_3 (haematite) in nanocrystals, analogous to the findings of Zhao et al. [9]. Chen et al. [10] used X-ray diffraction measurement of nanocrystalline ε-Fe up to 46 GPa to determine the value of the bulk modulus and its pressure derivative by analysing lattice parameter data. The compression behaviour of Rb_3C_{60} was first measured by X-ray diffraction under hydrostatic pressure up to 2.8 GPa in a diamond anvil cell at 300 K by Zhou et al. [11] and by Ludwig et al. [12] up to 6 GPa by a similar technique. Examination of previous EOS studies on Rb_3C_{60} with a diamond anvil cell showed that the technique has limited accuracy in the pressure range up to 1.5 GPa [13]. Diederichs et al. [14] performed neutron diffraction studies of the compressibility of this material and found that it was transformed to the nanoclinic baddeleyite structure at 20–30 GPa, which is higher than the corresponding pressure range for the bulk material.

Although experimental studies have been performed to determine the high-pressure behaviour of nanomaterials, theoretical work is lacking. We therefore present a simple theoretical method for studying the high-pressure behaviour of nanomaterials. The study, based on EOS at high pressure, permits interpolation and extrapolation to the regions for which adequate experimental data are not available and hence may be helpful for planning high-pressure experiments.

2. Method

Sharma and Kumar [15] published an equation for determining the effect of pressure on nanomaterials, in which pressure, P, is a function of the relative change in volume $(1 - V/V_0)$:

$$P = A_0 + A_1\left(1 - \frac{V}{V_0}\right) + A_2\left(1 - \frac{V}{V_0}\right)^2 \tag{1}$$

Kholiya [17] showed that a good approximation of expanding pressure on nanomaterials in powers of density up to the quadratic term is provided by:

$$P = A_0 + A_1\left(\frac{V}{V_0}\right)^{-1} + A_2\left(\frac{V}{V_0}\right)^{-2}, \tag{2}$$

where $V/V_0 = \rho_0/\rho$, and V_0, ρ_0 are the zero pressure values of volume V and density ρ, respectively, and A_0, A_1 and A_2 are constants at a particular temperature. Consideration of other higher-order terms of density or relative volume change involves second- and other higher-order pressure derivatives of the bulk modulus in the EOS, which are generally not available in the literature, especially for nanomaterials. The constants A_0, A_1 and A_2 can be determined from the following initial boundary conditions:

(i) $B_T = -V(dP/dV)$ and at $P = 0$, $V = V_0$, $B_T = B_0$
(ii) $B'_T = dB_T/dP$ and at $P = 0$, $V = V_0$, $B'_T = B'_0$
(iii) At $P = 0$, $V = V_0$, and the right-hand side in all these equations must be zero.

Applying these conditions in Eq. (1) we have:

$$A_0 = 0, \quad A_1 = B_0 \quad \text{and} \quad A_2 = \frac{B_0(B'_0 + 1)}{2}$$

Substituting these values, Eq. (1) becomes:

$$P = B_0\left[\left(1 - \frac{V}{V_0}\right) + \left(\frac{B'_0 + 1}{2}\right)\left(1 - \frac{V}{V_0}\right)^2\right] \tag{3}$$

This is the Shanker equation of state and may also be derived by the Gruneisen theory of thermal expansion

Table 1
Input parameters used to study compression behaviour in EOS models.

Material	B_0 (GPa)	B'_0	References
3C-SiC	245	2.9	[1]
$Zr_{0.1}Ti_{0.9}O_2$	213	17.9	[2]
CuO	81	4	[3]
AlN	321	4	[4]
TiO_2 (anatase)	243	4	[6]
TiO_2 (rutile)	211	8	[7]
α-Fe_2O_3	336	4	[8]
γ-Fe_2O_3	374	4	[9]
ε-Fe	179	3.6	[10]
Rb_3C_{60}	17.35	3.9	[11]

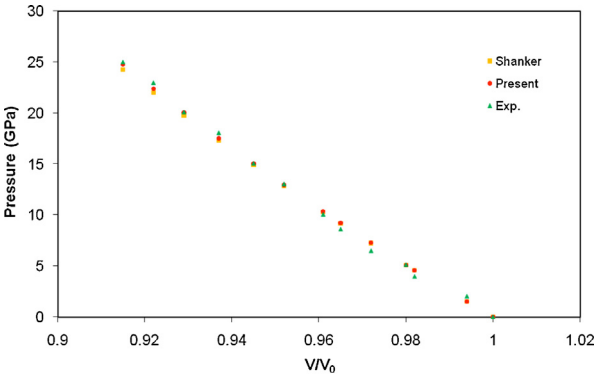

Fig. 1. Compression behaviour of 3C-SiC.
Experimental points are from Ref. [1].

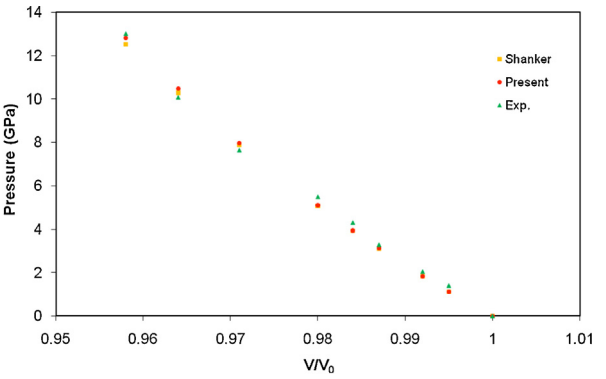

Fig. 2. Compression behaviour of $Zr_{0.1}Ti_{0.9}O_2$.
Experimental points are from Ref. [2].

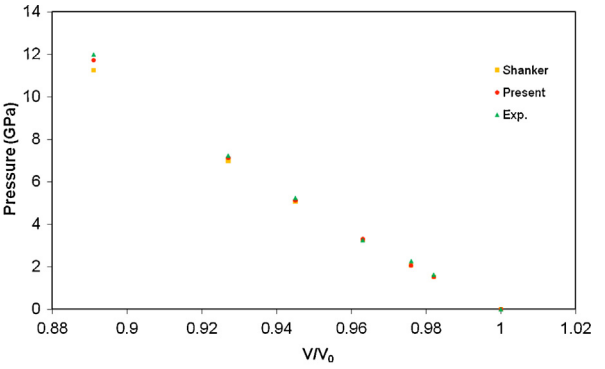

Fig. 3. Compression behaviour of CuO.
Experimental points are from Ref. [3].

[16]. Thus, the Sharma and Kumar formulation reproduces the Shanker EOS.

Applying boundary conditions in Eq. (2), we get:

$$A_0 = \frac{B_0(B_0' - 3)}{2}, \quad A_1 = -B_0(B_0' - 2)$$

$$\text{and} \quad A_2 = \frac{B_0(B_0' - 1)}{2}$$

By substituting these values, Eq. (2) becomes:

$$P = \frac{B_0}{2}\left[(B_0' - 3) - 2(B_0' - 2)\left(\frac{V}{V_0}\right)^{-1} + (B_0' - 1)\left(\frac{V}{V_0}\right)^{-2}\right] \tag{4}$$

Kholiya [17] showed that Eq. (4) satisfactorily explains the high-pressure elastic behaviour of carbon nanotubes and gives results similar to those of the Davis–Gordon EOS [18].

In the present study, we compared Eq. (4) with that of Sharma and Kumar (Shanker EOS) for a number of nanomaterials previously studied by those authors [15].

3. Results and discussion

The input parameters B_0 and B_0' used to study the compression behaviour in EOS models are listed in Table 1. The pressures for different compressions with these input parameters were calculated from Eqs. (3) and (4) for the nanomaterials 3C-SiC, $Zr_{0.1}Ti_{0.9}O_2$, CuO, AlN, TiO_2 (anatase), TiO_2 (rutile), α-Fe_2O_3, γ-Fe_2O_3, ε-Fe and Rb_3C_{60}. The results obtained are shown in Figs. 1–10, with the experimental data for comparison. The values calculated from Eq. (4) can be seen to be closer to the experimental values than those from Eq. (3), and the experimental data show only small differences from the calculated values for the nanomaterials studied. Kumar's equation also gives results within experimental uncertainty, as laboratory-measured P–V data are often subject to pressure calibration errors; however, the small difference between the values calculated from Kumar's equation and from Kholiya's equation are due

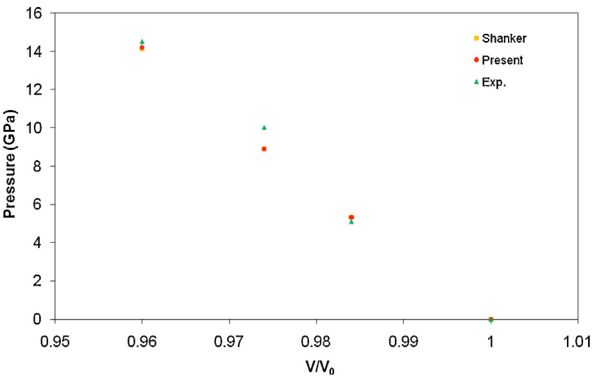

Fig. 4. Compression behaviour of AlN.
Experimental points are from Ref. [4].

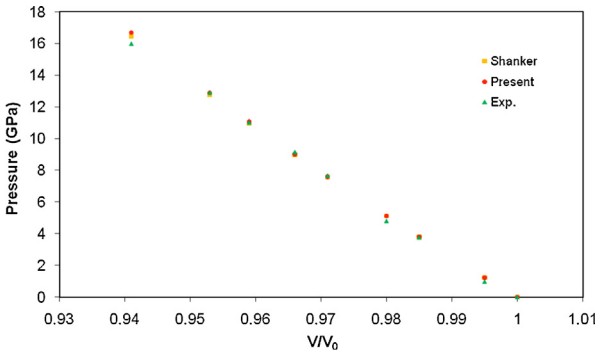

Fig. 5. Compression behaviour of TiO_2 (anatase). Experimental points are from Ref. [6].

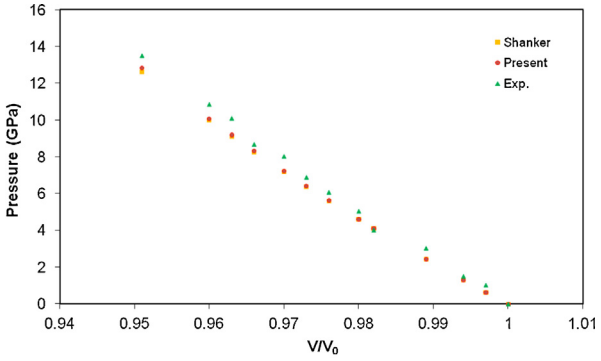

Fig. 6. Compression behaviour of TiO_2 (rutile). Experimental points are from Ref. [7].

to the fact that experimental data were available only up to low levels of compression, and the difference becomes large as compression increases, e.g. for 3C-SiC at $(V/V_0) = 0.6$, the pressure is 174.44 GPa with Kumar's and 266.78 GPa with Kholiya's equation. To extrapolate data for the region in which experimental data are not available, we require a model that is also valid in the high-pressure range. In Kumar's equation, (V/V_0) becomes zero at pressure $B_0[1 + ((B_0' + 1)/2)]$,

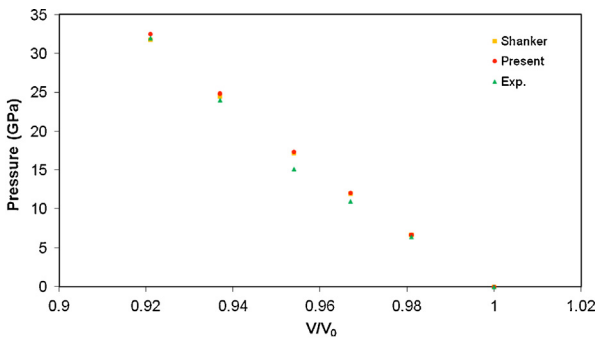

Fig. 7. Compression behaviour of α-Fe_2O_3. Experimental points are from Ref. [8].

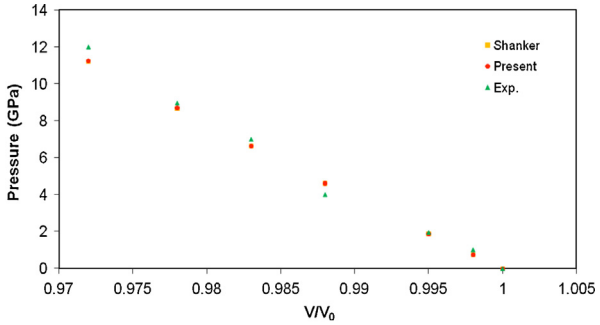

Fig. 8. Compression behaviour of γ-Fe_2O_3. Experimental points are from Ref. [9].

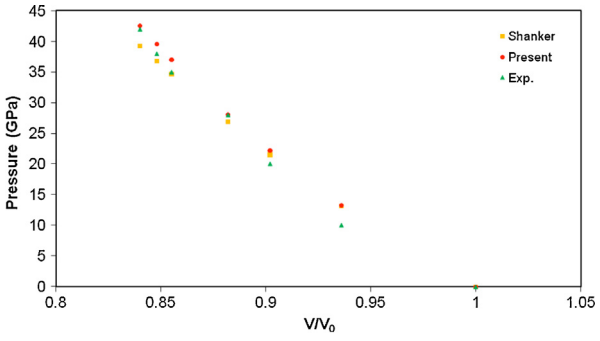

Fig. 9. Compression behaviour of ε-Fe. Experimental points are from Ref. [10].

i.e. finite pressure, while in our equation (V/V_0) becomes zero at infinite pressure. Thus, our equation gives valid results in the high-pressure range and can be used to extrapolate data to a high-pressure regime. Furthermore, Kumar's equation does not take into account the basic law of thermodynamics of solids, that the bulk modulus should approach infinity as (V/V_0) becomes zero. If the bulk modulus is given by $B = -V(dP/dV)$, the

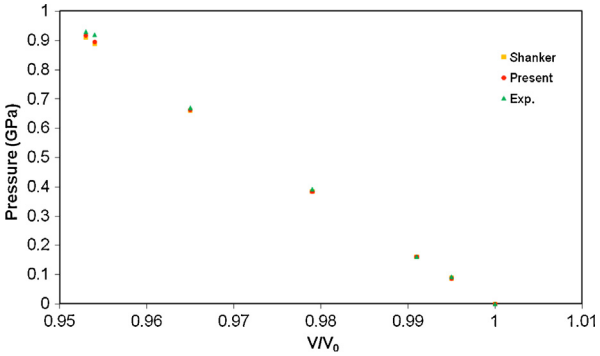

Fig. 10. Compression behaviour of Rb_3C_{60}. Experimental points are from Ref. [11].

expression for the bulk modulus from Eqs. (3) and (4) becomes:

$$B = B_0 \left(\frac{V}{V_0}\right)\left[1 + (B_0' + 1)\left\{1 - \frac{V}{V_0}\right\}\right] \quad (5)$$

$$B = B_0(B_0' - 2)\left(\frac{V}{V_0}\right)^{-1}\left[\left(\frac{B_0' - 1}{B_0' - 2}\right)\left(\frac{V}{V_0}\right)^{-1} - 1\right] \quad (6)$$

Eq. (5) indicates that with Kumar's formulation (Shanker EOS), the bulk modulus becomes zero when (V/V_0) approaches zero, while the basic law of thermodynamics indicates that the bulk modulus should approach infinity as (V/V_0) becomes zero. In Eq. (6), substitution of (V/V_0) by zero makes the bulk modulus infinity. Hence, our equation, developed by extending pressure in powers of density up to the quadratic term, satisfies the basic laws of the thermodynamics of solids.

4. Conclusions

Our equation, developed by extending pressure in powers of density up to the quadratic term, might be useful for studying the high-pressure compression behaviour of solids and especially nanomaterials, for which it gives results close to experimental data. The major advantage of this equation is that it follows the basic laws of thermodynamic with regard to relations at high pressure and hence permits extrapolation to regions for which experimental data are not available. The equation may therefore be helpful for planning high-pressure experiments on the compression behaviour of nanomaterials.

References

[1] J. Liu, C. Jin, J. Chen, J. Hu, Anomalous dynamical charge change behavior of nanocrystalline 3C-SiC upon compression, J. Am. Ceram. Soc. 87 (2004) 2291.

[2] E. Holbig, L. Dubrovinsky, G.S. Neumann, V. Prakapenka, V. Swamy, Compression behavior of Zr-doped nanoanatase, Z. Naturforsch 61 (b) (2006) 1577.

[3] Z. Wang, V. Pischedda, S.K. Saxena, P. Lazor, X-ray diffraction and Raman spectroscopic study of nanocrystalline CuO under pressures, Solid State Commun. 121 (2002) 275.

[4] Z. Wang, K. Tait, Y. Zhao, D. Schiferl, C. Zha, H. Uchida, R.T. Downs, Size-induced reduction of transition pressure and enhancement of bulk modulus of A1N nanocrystals, J. Phys. Chem. B 108 (2004) 11506.

[5] L.H. Shen, X.F. Li, Y.M. Ma, K.F. Yang, W.W. Lei, Q.L. Cui, G.T. Zou, Pressure-induced structural transition in AIN nanowires, Appl. Phys. Lett. 89 (2006) 141903.

[6] V. Swamy, L.S. Dubrovinsky, N.A. Dubrovinskaia, A.S. Simionovici, M. Drakopoulos, V. Dmitriev, H.P. Weber, Compression behavior of nanocrystalline anatase TiO_2, Solid State Commun. 125 (2003) 111.

[7] J.S. Olsen, L. Gerward, J.Z. Jiang, High pressure behavior of nano titanium dioxide, High Press. Res. 22 (2002) 385.

[8] S.M. Clark, S.G. Prilliman, C.K. Erdonmez, A.P. Alivisatos, Size dependence of the pressure-induced γ to α structural phase transition in iron oxide nanocrystals, Nanotechnology 16 (2005) 2813.

[9] J. Zhao, L. Guo, J. Liu, Y. Yang, R.Z. Che, L. Zhou, High Bulk Modulus of Nanocrystal γ-Fe_2O_3 with chemical dodecyl benzene sulfonic decoration under high pressure, Chin. Phys. Lett. 17 (2000) 126.

[10] B. Chen, D. Penwell, M.B. Kruger, A.F. Yue, B. Fultz, Nanocrystalline iron at high pressure, J. Appl. Phys. 89 (2001) 4794.

[11] O. Zhou, Q. Zhu, J.E. Fischer, N. Coustel, G.B.M. Vaughan, P.A. Heiner, J.P.J. McCauley, A.B. Smith III, Compressibility of M_3C_{60} fullerene superconductors: relation between T_c and lattice parameter, Science 255 (1992) 833.

[12] H.A. Ludwig, W.H. Fietz, F.W. Hornung, K. Grube, B. Renker, G.J. Burkhart, The compressibility of Rb_3C_{60} derived by X-ray experiments under high pressure, Physica C 234 (1994) 45.

[13] J.S. Schilling, S. Klotz, in: D.M. Ginsberg (Ed.), Physical Properties of High Temperature Superconductor III, World Scientific, Singapore, 1992.

[14] J. Diederichs, J.S. Schilling, K.W. Herwig, W.B. Yelon, Dependence of the superconducting transition temperature and lattice parameter on hydrostatic pressure for Rb_3C_{60}, J. Phys. Chem. Solids 58 (1997) 123.

[15] U.D. Sharma, M. Kumar, Effect of pressure on nanomaterials, Physica B 405 (13) (2010) 2820.

[16] J. Shanker, S.S. Kushwah, P. Kumar, Theory of thermal expansivity and bulk modulus for MgO and other minerals at high temperatures, Physica B 233 (1997) 78.

[17] K. Kholiya, High pressure isothermal equation of state for nanomaterials, Indian J. Phys. 87 (2013) 339.

[18] L.A. Davis, R.B. Gordon, Compression of mercury at high pressure, J. Chem. Phys. 46 (1967) 2650.